Supplement of Atmos. Meas. Tech., 19, 6159–6169, 2026
https://doi.org/10.5194/amt-19-6159-2026-supplement

Atmospheric Measurement Techniques
Open Access
EGU

Supplement of

Good performance of low-cost fast-response carbon dioxide sensor based on intercomparison with the standard eddy-covariance system

Üllar Rannik et al.

Correspondence to: Timo Vesala (timo.vesala@helsinki.fi)

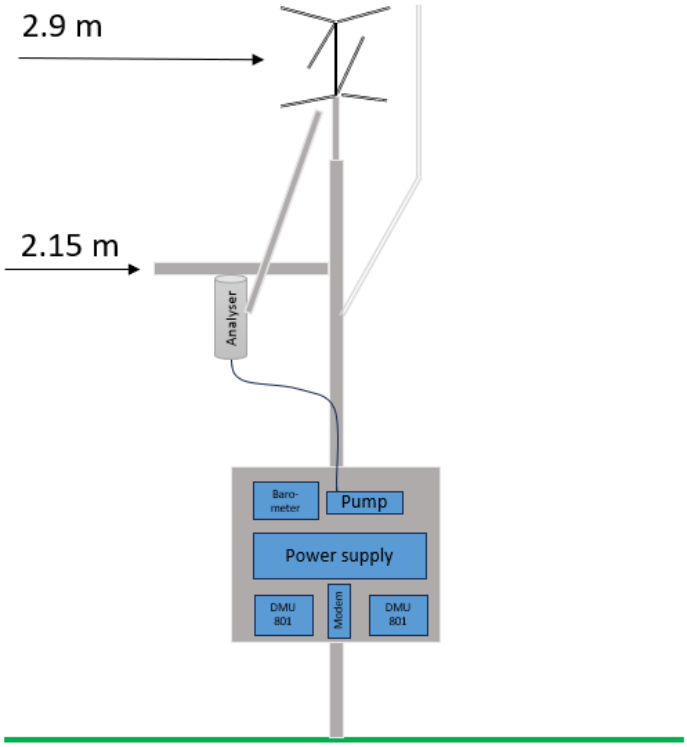

Figure S1: Schematic diagram of the prototype EC measurement setup. The rod rising on the level of the anemometer is a 4G antenna. The prototype gas analyser is located at a horizontal bar at 2.15 m from the ground. A heated sampling line of 70 cm length was used to suck air from close the anemometer to the prototype analyser. Instrumental box contained the pump, Vaisala digital barometer, power supply unit with fuses, Vaisala DMU801 data loggers and an internet modem.

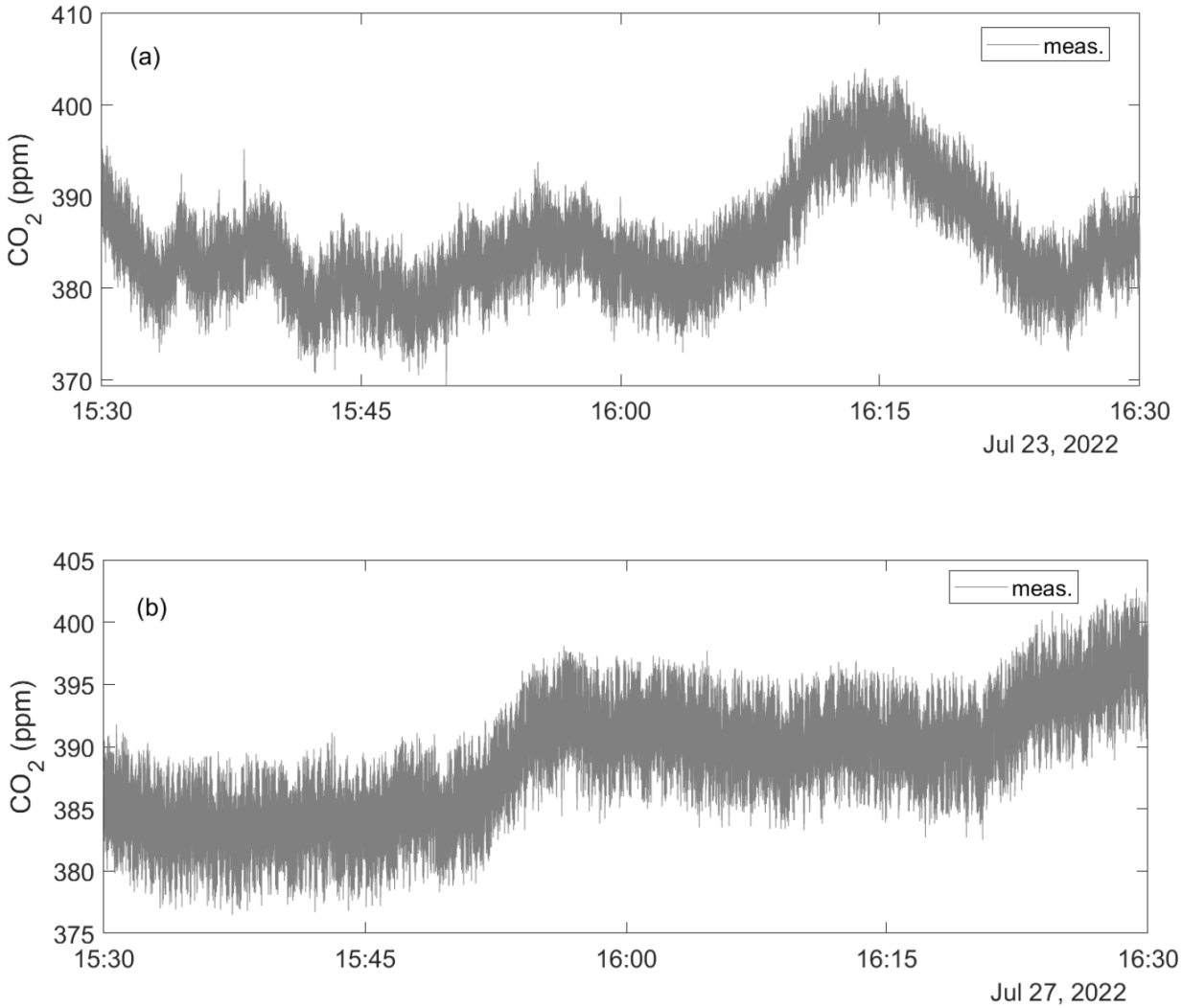

Figure S2 Examples of measured CO_2 mixing ratios after the software update on 21 July 2022. (a) 23 July and (b) 27 July from 15:30 till 16:30.

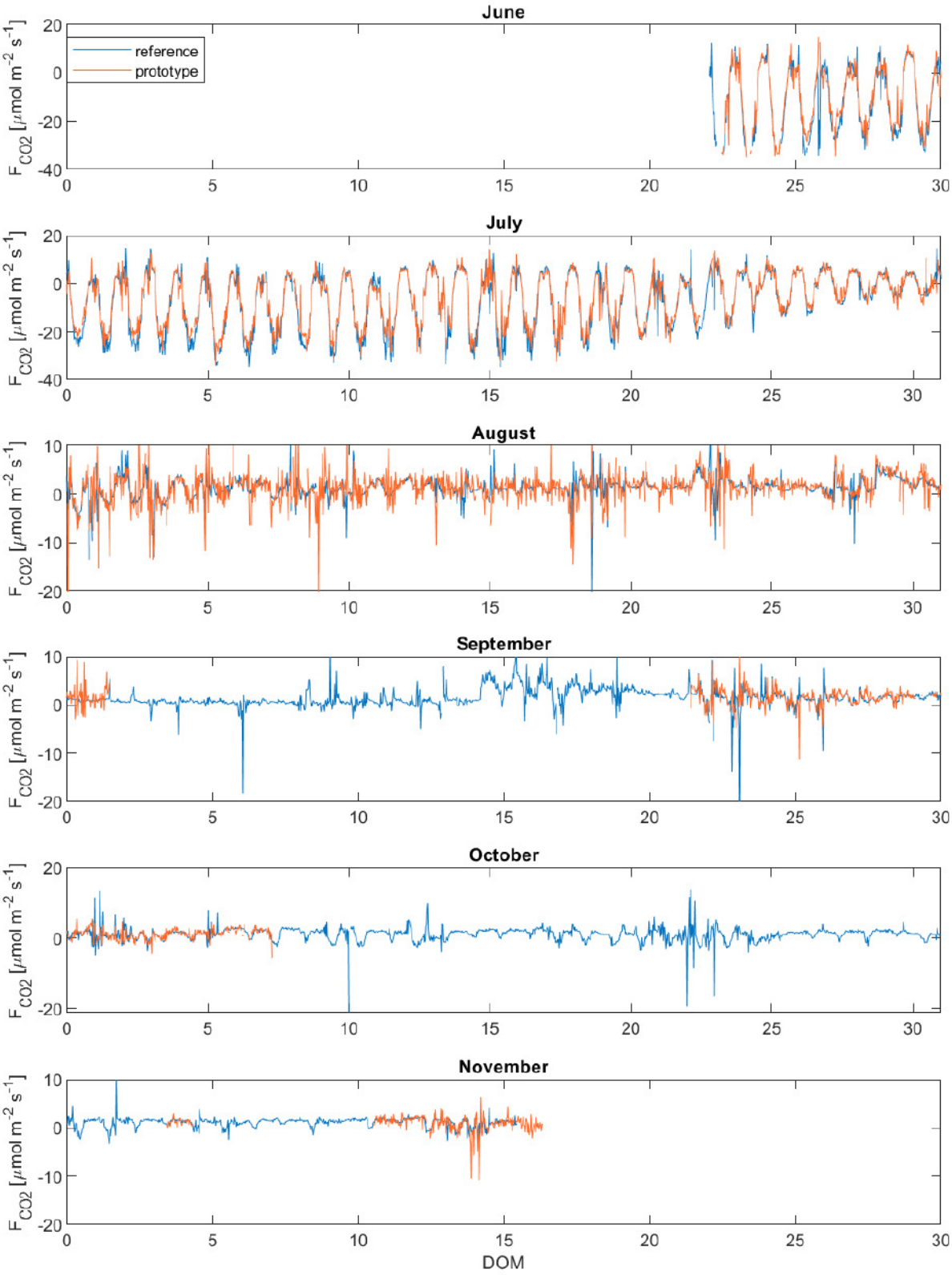

Figure S3: CO_2 fluxes available from the field measurements in June-November 2022.

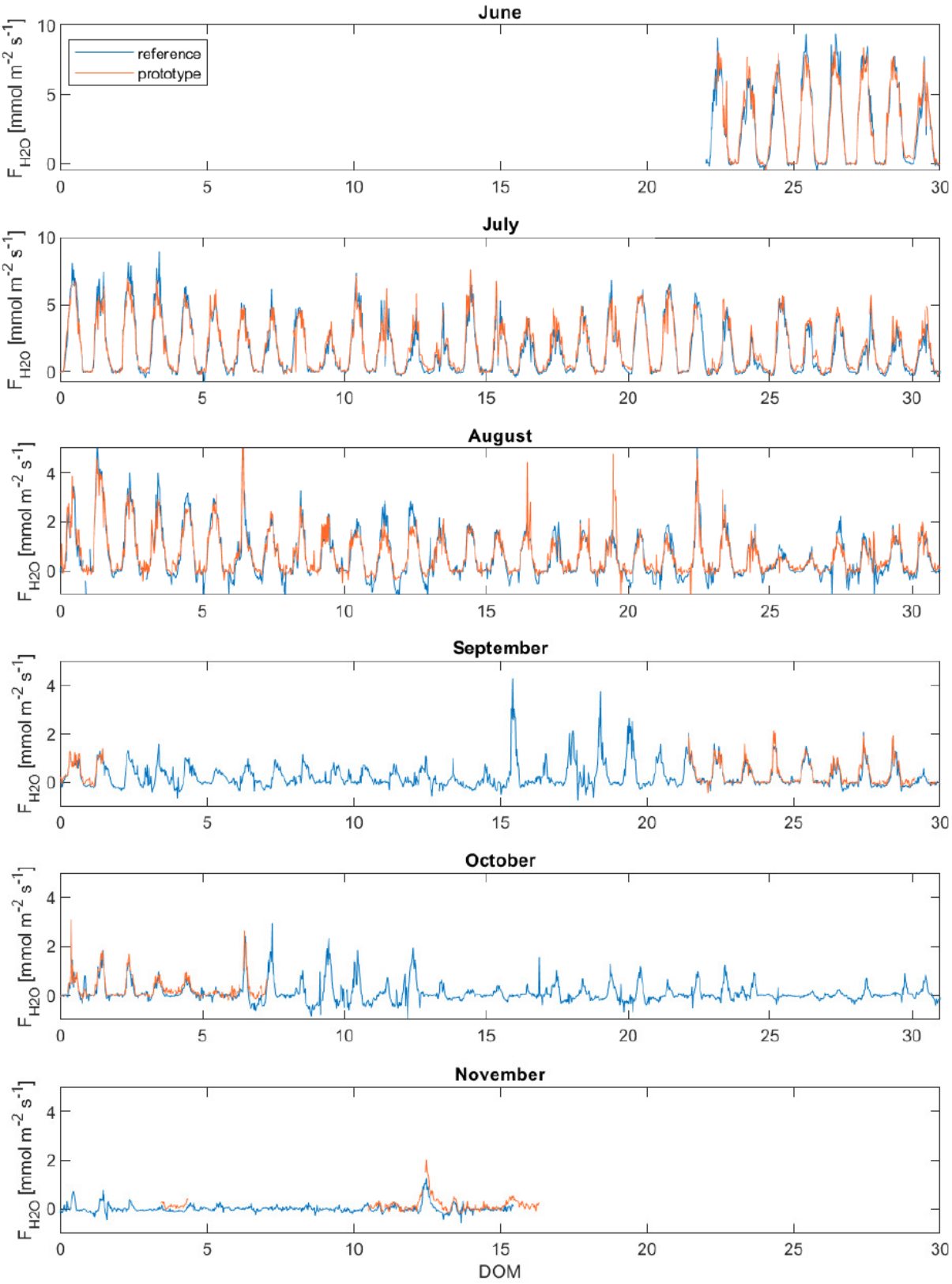

Figure S4: H_2O fluxes available from the field measurements in June-November 2022.

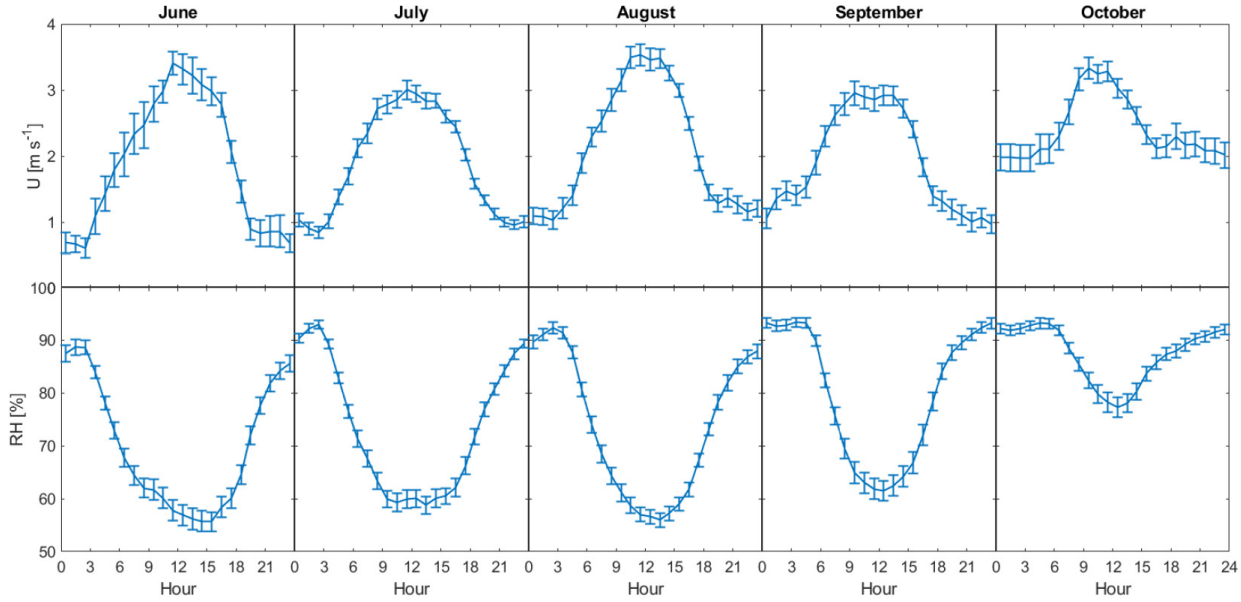

Figure S5: Monthly mean diurnal variations of wind speed and RH in June-October 2022.

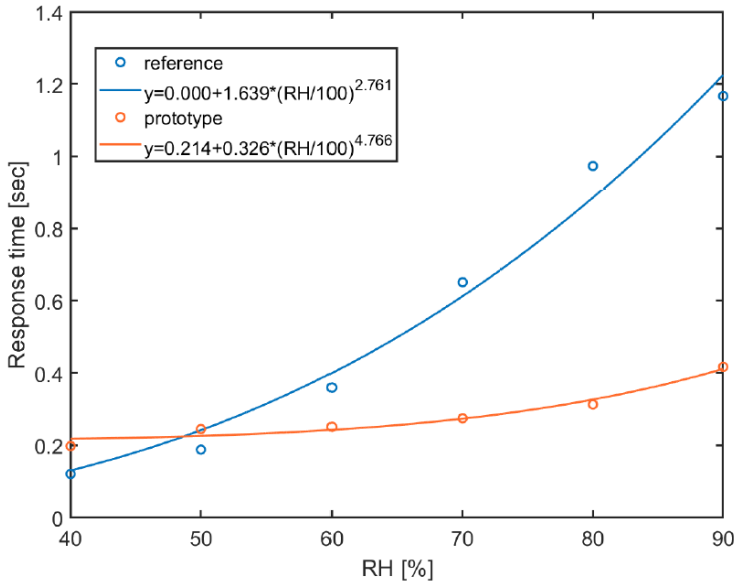

Figure S6: Relative humidity dependence of system response time for H_2O identified for the period June-July 2022. In response times calculation visual inspection of time series and calculated spectra was used to guarantee reliable results.

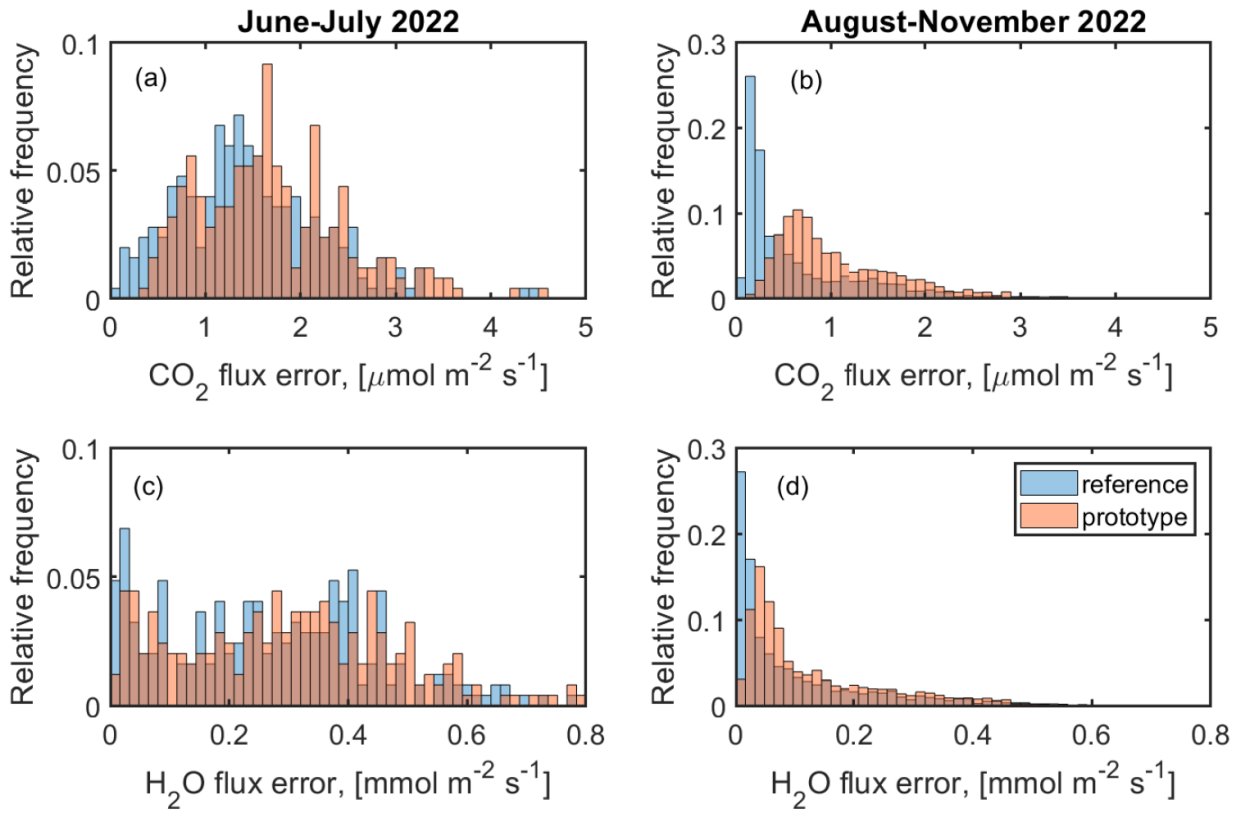

Figure S7: Histograms of the flux random errors for the period with higher carbon assimilation rates in June-July for (a) CO_2 and (c) H_2O; and for the period with low carbon assimilation rates in August-November for (b) CO_2 and (d) H_2O.

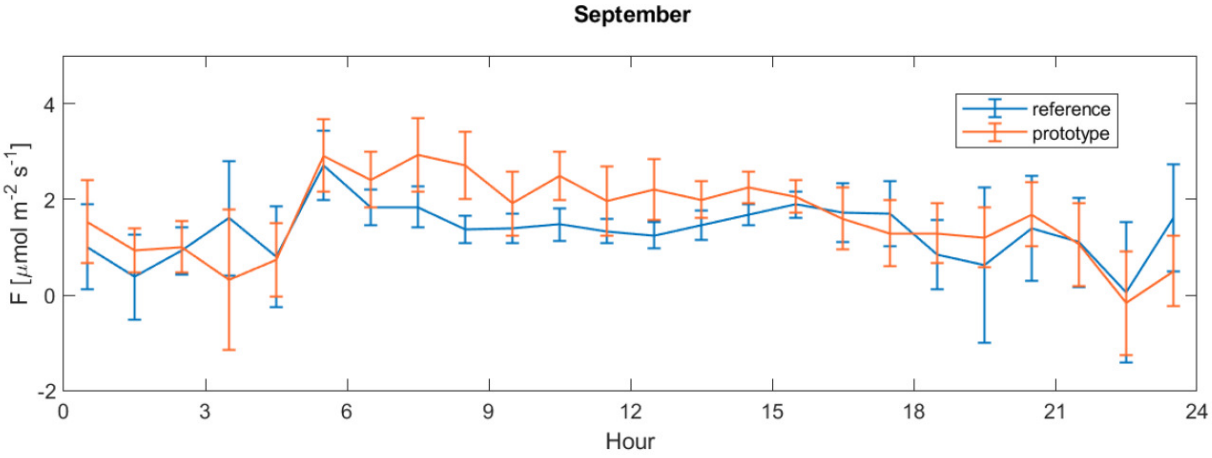

Figure S8: Diurnal variation of CO_2 for September 2022. The error bars represent 2 times the standard error of the hourly bin averages.